Genes & Diseases (2018) 5, 62–74

Available online at www.sciencedirect.com

ScienceDirect

journal homepage: http://ees.elsevier.com/gendis/default.asp

The development of a sensitive fluorescent protein-based transcript reporter for high throughput screening of negative modulators of lncRNAs

Zongyue Zeng [a,b], Bo Huang [a,b,c], Shifeng Huang [b,d], Ruyi Zhang [a,b], Shujuan Yan [a,b], Xinyi Yu [b,d], Yi Shu [b,e], Chen Zhao [b,d], Jiayan Lei [b,d], Wenwen Zhang [b,f], Chao Yang [b,e], Ke Wu [a,b], Ying Wu [b,g], Liping An [b,h], Xiaojuan Ji [b,e], Cheng Gong [b,i], Chengfu Yuan [b,j], Linghuan Zhang [b,e], Wei Liu [b,d], Yixiao Feng [b,d], Bo Zhang [b,h], Zhengyu Dai [b,k], Yi Shen [b,l], Xi Wang [a,b], Wenping Luo [b,m,n], Rex C. Haydon [b,d], Hue H. Luu [b,d], Lan Zhou [b,d], Russell R. Reid [b,o], Tong-Chuan He [a,b,*], Xingye Wu [b,d,**]

[a] *Ministry of Education Key Laboratory of Diagnostic Medicine and School of Laboratory Medicine, Chongqing Medical University, Chongqing, 400016, China*
[b] *Molecular Oncology Laboratory, Department of Orthopaedic Surgery and Rehabilitation Medicine, The University of Chicago Medical Center, Chicago, IL, 60637, USA*
[c] *Department of Clinical Laboratory Medicine, The Second Affiliated Hospital of Nanchang University, Nanchang, 330006, China*
[d] *Departments of Clinical Laboratory Medicine, General Surgery, Orthopedic Surgery, Nephrology, and Cardiology, The First Affiliated Hospital of Chongqing Medical University, Chongqing, 400016, China*
[e] *The Children's Hospital, Chongqing Medical University, Chongqing, 400014, China*
[f] *Department of Laboratory Medicine and Clinical Diagnostics, The Affiliated Yantai Hospital, Binzhou Medical University, Yantai, 264100, China*
[g] *Department of Immunology and Microbiology, Beijing University of Chinese Medicine, Beijing, 100029, China*
[h] *Key Laboratory of Orthopaedic Surgery of Gansu Province and the Department of Orthopaedic Surgery, The Second Hospital of Lanzhou University, Lanzhou, 730030, China*
[i] *Department of Surgery, The Affiliated Zhongnan Hospital of Wuhan University, Wuhan, 430071, China*

* Corresponding author. Molecular Oncology Laboratory, The University of Chicago Medical Center, 5841 South Maryland Avenue, MC 3079, Chicago, IL, 60637, USA. Fax: + 773 834 4598.
** Corresponding author. Department of General Surgery, The First Affiliated Hospital of Chongqing Medical University, Chongqing, 400016, China. Fax: + 86 23 8901 1172.
E-mail addresses: tche@uchicago.edu (T.-C. He), wuxingye19830221@126.com (X. Wu)
Peer review under responsibility of Chongqing Medical University.

https://doi.org/10.1016/j.gendis.2018.02.001

[j] *Department of Biochemistry and Molecular Biology, China Three Gorges University School of Medicine, Yichang, 443002, China*
[k] *Department of Orthopaedic Surgery, Chongqing Hospital of Traditional Chinese Medicine, Chongqing, 400021, China*
[l] *Department of Orthopaedic Surgery, Xiangya Second Hospital of Central South University, Changsha, 410011, China*
[m] *Chongqing Key Laboratory for Oral Diseases and Biomedical Sciences, Chongqing, 401147, China*
[n] *The Affiliated Hospital of Stomatology of Chongqing Medical University, Chongqing, 401147, China*
[o] *Department of Surgery, Laboratory of Craniofacial Biology and Development, Section of Plastic Surgery, The University of Chicago Medical Center, Chicago, IL, 60637, USA*

Received 6 January 2018; accepted 5 February 2018
Available online 21 February 2018

KEYWORDS
BiFP;
Green fluorescent protein;
High throughput screening;
lncRNA;
Noncoding RNA;
Transcript reporter assay

Abstract While the human genome is pervasively transcribed, <2% of the human genome is transcribed into protein-coding mRNAs, leaving most of the transcripts as noncoding RNAs, such as microRNAs and long-noncoding RNAs (lncRNAs), which are critical components of epigenetic regulation. lncRNAs are emerging as critical regulators of gene expression and genomic stability. However, it remains largely unknown about how lncRNAs are regulated. Here, we develop a highly sensitive and dynamic reporter that allows us to identify and/or monitor negative modulators of lncRNA transcript levels in a high throughput fashion. Specifically, we engineer a fluorescent fusion protein by fusing three copies of the PEST destruction domain of mouse ornithine decarboxylase (MODC) to the C-terminal end of the codon-optimized bilirubin-inducible fluorescent protein, designated as dBiFP, and show that the dBiFP protein is highly destabilized, compared with the commonly-used eGFP protein. We further demonstrate that the dBiFP signal is effectively down-regulated when the dBiFP and mouse lncRNA H19 chimeric transcript is silenced by mouse H19-specific siRNAs. Therefore, our results strongly suggest that the dBiFP fusion protein may serve as a sensitive and dynamic transcript reporter to monitor the inhibition of lncRNAs by microRNAs, synthetic regulatory RNA molecules, RNA binding proteins, and/or small molecule inhibitors so that novel and efficacious inhibitors targeting the epigenetic circuit can be discovered to treat human diseases such as cancer and other chronic disorders.

Introduction

Eukaryotic genomes are pervasively transcribed, but until recently the vast majority of the noncoding transcriptions were considered to be simply noise.[1–12] It is currently estimated that approximately <2% of the human genome is transcribed into mRNA, which leaves most of the transcribed human genome encoding RNA without known functions, or so-called noncoding RNAs (ncRNAs).[8,9,13] In fact, a recent comprehensive RNA-seq data mining study revealed a consensus human transcriptome of 91,013 expressed genes; and over 68% (58,648) of the genes were classified as long noncoding RNAs (lncRNAs), of which 79% were previously unannotated.[14] Furthermore, noncoding transcription units overlap with genes, indicating genomes are extensively interleaved.[15] Noncoding RNAs include the well-known ribosomal (r)RNAs, ribozymes, transfer(t)RNAs, small nuclear (sn)RNAs, telomere-associated RNAs(TERRA, TERC), as well as a plethora of far less characterized RNAs.[16] Based on their size, these ncRNAs are subdivided into two groups: small ncRNAs (<200 nt) and long ncRNAs [lncRNA (>200 nt)][10,13,16–24]. Small ncRNAs, such as microRNAs (miRs), small interfering RNAs (siRNAs), or PIWI-interacting RNAs (piRNAs) received much attention and were shown to mainly act as negative regulators of gene expression. In contrast, lncRNAs represent a more functionally diverse class of transcripts. The precise outcome depends on the relative orientation of the transcription units and whether two overlapping transcription events are contemporaneous or not, but generally involves chromatin-based changes.[15,17,25]

Emerging evidence suggests that epigenetic control of gene expression may play a major role in regulating many cellular processes.[12,14,18,26–32] As the epigenetic control of gene expression is a critical component of transcriptional regulation,[6,14,18,23,26,27] the deposition of epigenetic modifications is often guided by noncoding RNAs.[10,13,16–24] Although noncoding RNAs, including microRNAs and lncRNAs, have been most often implicated in post-transcriptional gene silencing, these molecules are now emerging as critical regulators of gene expression and genomic stability at the transcriptional level.[10,13,16,17,21–24] The complex and diverse functions of ncRNAs (esp. lncRNAs) are just starting to emerge, ranging from

regulating chromatin remodeling, gene transcription and translation, RNA stability, scaffolding, and innate immunity.[8,9,11,13,15,17,25] Thus, we are only beginning to understand the nature and extent of the involvement of ncRNAs in human diseases and there is great interest in therapeutic strategies to counteract these perturbations of ncRNAs.[33–35]

Nonetheless, the ncRNA field faces at least two formidable challenges: effective identification and functional annotation of ncRNAs (esp. lncRNAs). Currently, the identification of ncRNAs mainly relies on large-scale deep genome sequencing, improved epigenomic technologies and computational predictions. However, these approaches may be limited by the low expression level of ncRNAs, which is, on average, 10–20 times lower than the expression level of protein-coding genes. Furthermore, it becomes increasingly clear that lncRNA repertoires are subject to weak functional constraint and rapid turnover during vertebrate evolution.[36] Many lncRNAs do not exhibit the same pattern of high interspecies conservation as protein-coding genes.[11,25,36] The identification process is further complicated by the fact that one lncRNA usually targets multiple genes, vice versa. Thus, novel techniques are needed to investigate the biological functions and regulation of lncRNAs.

In this study, we sought to develop a highly sensitive and dynamic reporter that allows us to identify and/or monitor negative modulators of lncRNA transcript levels in a high throughput fashion. Even though various reporter systems have been developed for various gene regulation or drug selection studies,[37,38] sensitive reporters to assess the dynamic and real-time changes of lncRNA levels upon different inhibitor treatments are not available. An ideal reporter for assessing the decrease in lncRNA transcript level should have a short half-life yet high basal signal. Here, we engineer a fluorescent fusion protein by fusing three copies of the PEST destruction domain of mouse ornithine decarboxylase (MODC)[39] to the C-terminal end of the codon-optimized bilirubin-inducible fluorescent protein, designated as dBiFP, and show that dBiFP protein is highly destabilized and degradable, compared with the commonly-used eGFP. We further demonstrate that the dBiFP signal is effectively down-regulated when the dBiFP and mouse lncRNA H19 chimeric transcript is silenced by mouse H19-specific siRNAs. Thus, our results strongly suggest that the dBiFP fusion protein may serve as a sensitive yet dynamic transcript reporter to monitor the targeted inhibition of lncRNAs by microRNAs, RNA binding proteins, synthetic RNA molecules and small molecule inhibitors in a high throughput fashion.

Materials and methods

Cell culture and chemicals

Human colorectal cancer line HCT116 and HEK-293 were purchased from the American Type Culture Collection (ATCC, Manassas, VA). 293pTP and RAPA cells derived from HEK-293 cells as previously characterized.[40,41] All cell lines were maintained in Dulbecco's Modified Eagle Medium (DMEM) supplemented with 10% fetal bovine serum (FBS, Gemini Bio-Products, West Sacramento, CA), containing 100 U/ml penicillin and 100 μg/ml streptomycin, at 37 °C in 5% CO_2 as described.[42–44] Cycloheximide (CHX) and hygromycin B were purchased from Cayman Chemical (Ann Arbor, MI). Unless indicated otherwise, other reagents were purchased from Sigma–Aldrich (St. Louis, MO) or Thermo Fisher Scientific (Waltham, MA).

Codon optimization and expression of bilirubin-inducible fluorescent protein (BiFP)

As one of the first fluorescent proteins identified from vertebrates, UnaG (AB763906.1) is a bilirubin-binding fluorescent protein (BiFP) that was originally identified from Japanese eel muscle cells.[45] To facilitate the expression of this gene in human cells, we synthesized and humanized the gene through codon optimization (Genescript, Piscataway, NJ). The synthesized BiFP coding region was subcloned into pSEH retroviral vector, resulting in pSEH-BiFP, and verified by DNA sequencing. This vector was served as the template for generating various degradable versions of BiFP constructs.

Construction of pSEH-eGFP and pSEH-GLuc and their destabilized counterpart pSEH-eGFP-3modc and pSEH-GLuc-3modc vectors

The coding sequences of enhance GFP (eGFP) and Gaussia luciferase (GLuc) were PCR amplified using the Phusion High-Fidelity PCR Kit (New England Biolabs, Ipswich, MA) and cloned into the pSEH vector at the HindIII and SalI sites, resulting in pSEH-eGFP and pSEH-GLuc vectors, respectively. Three copies of the MODC destruction domain (see below) were added in-frame to the C-terminal ends of eGFP and GLuc, resulting in pSEH-eGFP-3modc and pSEH-GLuc-3modc vectors, respectively. All PCR amplified fragments were verified by DNA sequencing.

Generation of the destabilized/degradable BiFP (dBiFP) proteins with the MODC domain fused at the N- and/or C-termini of BiFP

To facilitate the generation of multiple copies of the PEST destruction domain (e.g., amino acids 422–461) of mouse ornithine decarboxylase (MODC),[39] the MODC coding sequence was repeated three times separated by linker sequences and synthesized as a gBlocks gene fragment (IDT, Coralville, Iowa). One to three copies of MODC sequence were then PCR amplified from the gBlocks fragment (Supplemental Table 1) and used to generate N- or C-terminal fusion proteins of BiFP. Specifically, the pSEH-BiFP-modc, pSEH -BiFP-2modc, and pSEH-BiFP-3modc vectors contain one, two and three copies of the MODC domain at the C-terminus of BiFP coding sequence, respectively. Accordingly, the pSEH-3modc-BiFP vector contains three copies of the MODC domain at the N-terminus of BiFP, was also designated as the pdBiFP-Linker vector (Supplemental Figure 1). All PCR amplified sequences were verified by DNA

sequencing. The primers used for cloning are listed in Supplemental Table 1. Details about the vector constructions are available upon request.

Construction of the dBiFP-based lncRNA H19 reporter pSEH-dBiFP-H19

The mouse lncRNA H19 was PCR amplified from the pSEB-H19[46], and subcloned into the XhoI and MluI sites of pSEH-BiFP-3modc (i.e., pdBiFP-Linker) (Supplemental Figure 1), resulting in pSEH-dBiFP-H19. The PCR amplified sequence was verified by DNA sequencing.

Generation and amplification of recombinant adenovirus expressing siRNAs targeting mouse lncRNA H19

Recombinant adenoviral vectors were constructed by using the AdEasy technology as described.[47,48] Briefly, three siRNA sites targeting mouse lncRNA H19 were simultaneously assembled to an adenoviral shuttle vector using the Gibson Assembly system as described,[49,50] followed by generation of recombinant adenoviruses in HEK-293, 293pTP or RAPA cells as described.[40,41] The resultant adenoviruses, designated as AdR-simH19, which also expresses RFP as a marker for monitoring infection efficiency. An analogous adenovirus expressing RFP only (Ad-RFP) was used as a mock virus control. For all adenovirus infections, polybrene (8 μg/mL) was added to the culture medium to enhance adenoviral infection efficiency.[51]

Retrovirus production and the establishment of HCT116 stable lines

The retrovirus packaging and infection were carried out as described.[52] Briefly, the pSEH series retroviral vectors were co-transfected with the packaging plasmid pCL-AMPHO into HEK-293 cells. The packaged retrovirus supernatants were collected at 36 h, 48 h, 60 h and 72 h, respectively. The supernatants were filtered and used for 3—4 rounds of infection of subconfluent HCT116 cells.[52] At 24 h post the last round of infection, the infected HCT116 cells were selected in the presence of hygromycin B (0.3 mg/ml) for 5—7 days.

Protein turnover and fluorescence intensity analysis

To determine protein turnover, the cells were treated with cycloheximide (CHX) at a final concentration of 100 μg/ml as described.[53] The fluorescence intensity was recorded at various time points and then quantified by using the Image J software. Average fluorescence intensity = Integrated density/Area. The experiments were done in triplicate.

Gaussia luciferase assay

The GLuc assay was carried out as described.[54—56] Briefly, the GLuc activity was detected using BioLux® Gaussia Luciferase Assay Kit (New England Biolabs) according to the manufacturer's instructions. Briefly, the GLuc assay solution was prepared by freshly mixing 5 μl of BioLux GLuc Substrate, 80 μl of BioLux Gluc Stabilizer, and 0.5 ml of BioLux GLuc Assay Buffer. 20 μl of the GLuc assay solution were added to each sample, followed by incubating at room temperature for 35—40sec before measurement. Each assay condition was done in triplicate.

RNA isolation and touchdown quantitative Real-Time PCR (TqPCR)

Total RNA was isolated with NucleoZOL (Takara Bio USA, Mountain View, CA) according to the manufacturer's instructions. Reverse transcription reactions were done using hexamer and M-MuLV Reverse Transcriptase (New England Biolabs, Ipswich, MA). The cDNA products were diluted 20- to 100-fold and used as PCR templates. Primer3 Plus program were used to design the qPCR primer.[57] The qPCR analysis was carried out using our recently optimized TqPCR protocol.[58] Briefly, the SYBR Green qPCR reactions (Bimake, Houston, TX) were set up according to manufacturer's instructions. The cycling program was modified by incorporating 4 cycles of touchdown steps prior to the regular cycling program as described[58]: 95 °C × 3 min for one cycle; 95 °C × 20 s, 66 °C × 10 s for 4 cycles, with 3 °C decrease per cycle; followed by 95 °C × 10 s, 55 °C × 15 s, 70 °C × 1 s for 40 cycles, followed by plate read. All reactions were done in triplicate. GADPH was used as a reference gene. All sample values were normalized to *GADPH* expression by using the $2^{-\Delta\Delta Ct}$ method. The qPCR primer sequences are listed in the Supplemental Table 1.

Statistical analysis

All quantitative experiments were performed in triplicate and/or repeated in three independent batches of experiments. Data were expressed as mean ± standard deviation (SD). The one-way analysis of variance was used to analyze statistical significance. A value of $p < 0.05$ was considered statistically significant.

Results

Multimerized MODC PEST domains can destabilize Gaussia luciferase (GLuc) and to a lesser extent, eGFP

An ideal sensitive inhibition reporter should have a high basal signal, which can be reduced rapidly to reflect the dynamic changes upon inhibition. Although the PEST destruction domain (e.g., amino acids 422—461) of mouse ornithine decarboxylase (MODC) has been used to destabilize several reporters, including eGFP,[39] the destabilized reporters such as eGFP remain relatively stable and fail to reflect the dynamic changes upon various treatments.

Here, we sought to test whether adding multiple copies of the MODC destruction domain to eGFP or GLuc would further destabilize the reporter. Thus, we added three copies of MODC domain to the C-terminal end of eGFP and generated the eGFP-3modc construct (Figure 1A). We found that the GFP signal of the eGFP-3modc fusion protein was

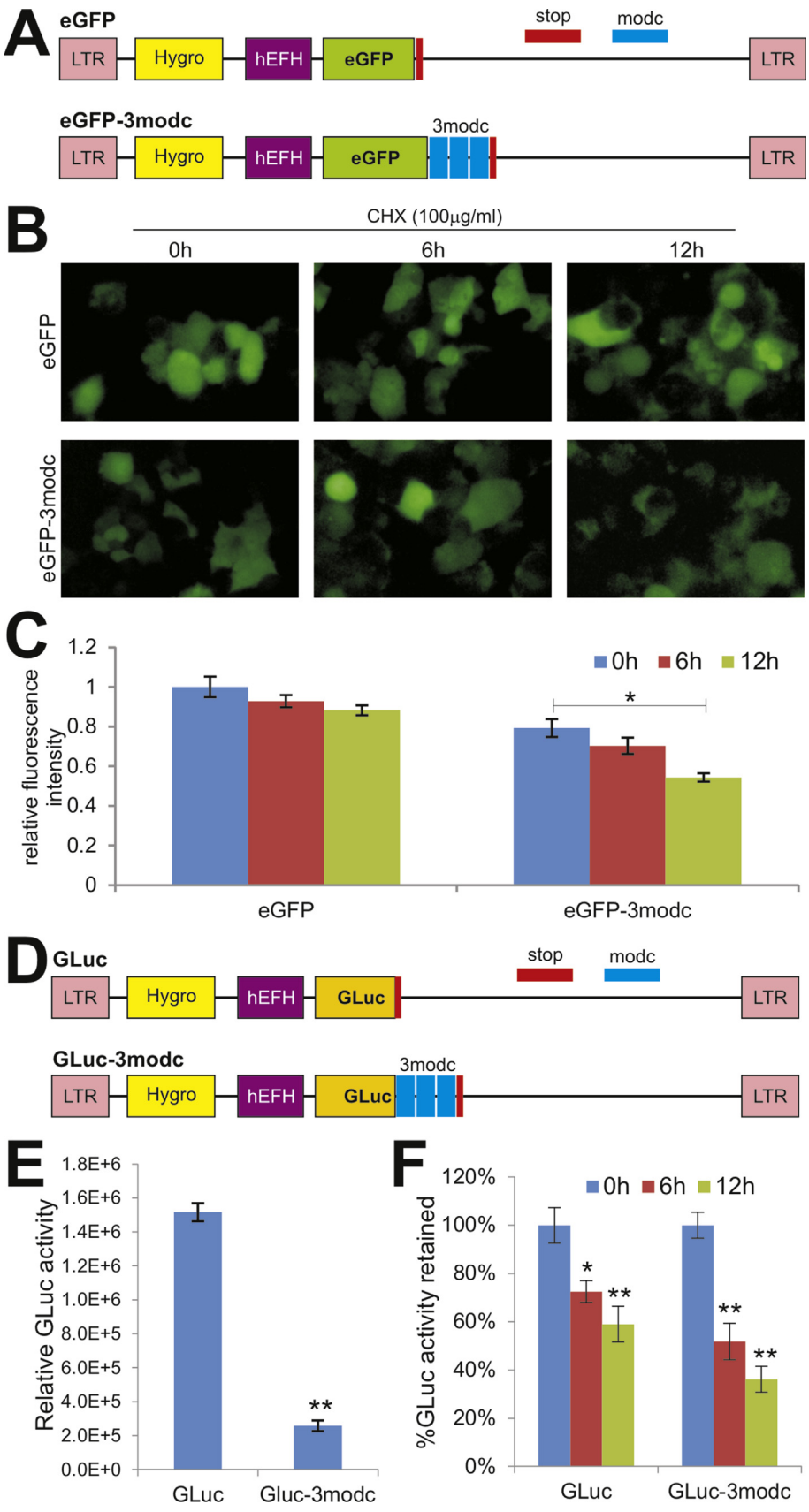

Figure 1 Fusion proteins of eGFP and Gaussia luciferase (GLuc) with multiple copies of the MODC PEST domain exhibit varied instabilities. (**A**) Schematic representation of the construction of eGFP-3modc C-terminal fusion and its control eGFP vectors. Both constructs were generated on the basis of our homemade pSEH retroviral vector, yielding pSEH-eGFP and pSEH-eGFP-3modc. LTR,

slightly decreased, compared with that of eGFP, and showed a significant decrease at 12 h after cycloheximide treatment (Fig. 1B). Quantitative analysis revealed that the average GFP signal of the eGFP-3modc stable cells was approximately 79.3% of the eGFP group at basal level (Fig. 1C). However, at 12 h after cycloheximide treatment, the average GFP signal of the eGFP-3modc stable cells only dropped to 68.6% of its basal signal (e.g., at 0 h) (Fig. 1C), indicating that the fusion protein was still rather stable and may not be used as an ideal dynamic reporter.

We also added three copies of MODC domain to the C-terminal end of GLuc and made the GLuc-3modc construct (Fig. 1D), and found that the basal GLuc activity of the GLuc-3modc fusion protein was significantly decreased to 17.1% of the GLuc group ($p < 0.01$) (Fig. 1E). At 12 h after cycloheximide treatment, the GLuc activity of the GLuc-3modc fusion was drastically reduced to 36.1% of its basal level (i.e., at 0 h) ($p < 0.01$) (Fig. 1F). These results are consistent with the fact that GLuc is a relatively high-lived protein, and the addition of MODC destruction domain may further destabilize GLuc protein, suggesting that the GLuc-3modc fusion may serve as a sensitive and dynamic reporter. However, the low throughput nature of GLuc assay may prevent its utility for large scale high throughput screening of negative regulators or inhibitors.

Codon-optimized bilirubin-inducible fluorescent protein (BiFP) can be engineered as a highly destabilized reporter

As eGFP is a rather stable protein, we explored alternative GFPs. Recently, a bilirubin-binding fluorescent protein (BiFP) (aka, UnaG) was identified in Japanese eel muscle cells, representing one of the first fluorescent proteins found in vertebrates[45] (Fig. 2A-ab). In order to facilitate the expression of this gene in human cells, we synthesized a humanized version of BiFP through codon optimization (Fig. 2A—c). We found that BiFP can be transiently expressed effectively in human cells, and robust green fluorescent signal was detectable at as early as 12 h post transfection (Fig. 2B).

To determine whether the MODC destruction domain was able to destabilize the BiFP protein, we engineered three BiFP retroviral constructs, which contained one, two and three copies of MODC domain fused to the C-terminus of BiFP, resulting in BiFP-modc, BiFP-2modc, and BiFP-3modc, respectively (Fig. 3A). When these BiFP fusion constructs were stably expressed in HCT116 cells, we found the basal green fluorescence signal intensity was comparable among the three BiFP fusion proteins and the non-fusion BiFP control, although there was a trend of decreasing signal with the increase in the copy numbers of MODC domain (Fig. 3B). However, when the protein synthesis was inhibited by CHX, GFP signal decreased significantly in BiFP-2modc and BiFP-3modc at as early as 6 h post CHX treatment, and became more pronounced at 12 h post CHX treatment, compared with that of the BiFP non-fusion control (Fig. 3B). Quantitative analysis further confirmed this trend and revealed that the green fluorescence signal intensity of the BiFP-3modc fusion protein decreased to 24.1% of its basal level, or ~76% decrease, at 12 h post CHX treatment ($p < 0.01$) (Fig. 3C). Collectively, these results indicate that BiFP may be effectively destabilized by multimerized MODC destruction domain.

The C-terminal fusion, not N-terminal fusion, of MODC domain is more effective to destabilize BiFP

We further tested whether the N-terminal fusion of MODC would destabilize BiFP more effectively than that of the C-terminal fusion. We added three copies of MODC domain at the N-terminal end of the BiFP protein, resulting in 3modc-BiFP (Fig. 4A). When both N-terminal and C-terminal fusion constructs were stably expressed in HCT116 cells, we found the basal green fluorescence signal levels were comparable for both constructs, as well as for the non-fusion BiFP control (Fig. 4B). However, upon CHX treatment, the green fluorescence signal decreased more precipitately in the C-terminal fusion BiFP-3modc cells than that of the N-terminal fusion construct (Fig. 4B). Quantitative analysis revealed that the green fluorescence signal intensity in BiFP-3modc stable cells decreased to 24.9% of its basal level (e.g., at 0 h), or ~75% decrease, at 12 h post CHX treatment ($p < 0.01$), compared with 58.9% of 3modc-BiFP's basal level, or ~42% decrease, at the same time point (Fig. 4C). Collectively, the above results demonstrate that the C-terminal fusion protein BiFP-3modc exhibits a high basal level of green fluorescence signal, which can be rapidly down-regulated upon the inhibition of protein synthesis. Thus, the BiFP-3modc fusion protein may serve as a sensitive and dynamic fluorescent protein reporter due to its shortened half-life. To simplify the nomenclature, we designated the BiFP-3modc fusion protein as the

long terminal repeat for MSCV retrovirus; Hygro, hygromycin B resistance gene; hEFH, a hybrid promoter consisting of human EF1α promoter and HIV enhancer; eGFP, enhanced green fluorescent protein; stop, stop codon; 3modc, three copies of the PEST-containing degradation domain of mouse ornithine decarboxylase. (**B**) The fluorescence signal of the eGFP-3modc fusion after cycloheximide (CHX) treatment. The retroviral vectors were used to make stable cell lines of HCT116 cells after hygromycin selection. The stable lines were seeded at subconfluency and treated with cycloheximide (100 μg/ml). Fluorescence signals were recorded at the indicated time points. Representative images are shown. (**C**) Quantitative analysis of the fluorescence intensity in the samples prepared in (B). "*" $p < 0.05$ compared with GFP signal between 0 h and 12 h. (**D**) Schematic representation of the construction of GLuc-3modc fusion and its control GLuc vectors. Both constructs were retroviral vectors, namely pSEH-GLuc and pSEH-GLuc-3modc. (**E**). The retroviral vectors were used to make stable HCT116 cell lines, as described in (B). Basal GLuc activity was measured. "**" $p < 0.01$, compared with non-fusion GLuc control line. (**F**). GLuc activity retained after CHX treatment. The GLuc and GLuc-3modc stable lines were treated with CHX (100 μg/ml). GLuc activities were measured at the indicated time points. "*$p < 0.05$, "**"$p < 0.01$, compared with the GLuc activity at 0 h time point.

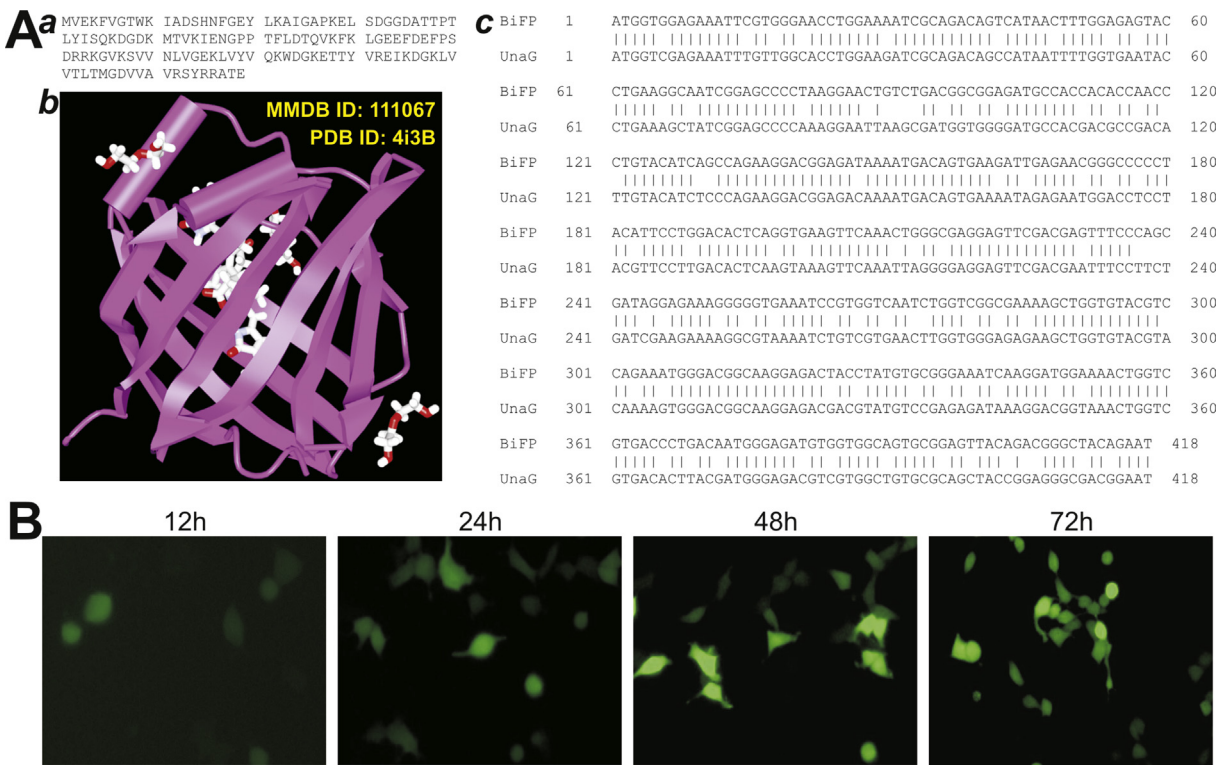

Figure 2 The construction and expression of codon-optimized bilirubin-inducible fluorescent protein (BiFP). (**A**) Codon optimization of BiFP. The protein sequence of BiFP (aka, UnaG) (***a***) and its crystal structure (***b***) were previously described in reference[45]. As the original gene was identified from Japanese eel muscle cells, we humanized the gene; and the codon optimized BiFP and original UnaG coding sequences were compared and shown in (***c***). (**B**) Effective expression of BiFP in HEK-293 cells. The codon optimized BiFP was subcloned into pSEH vector and transiently transfected into HEK-293 cells. The green fluorescence signal was recorded at the indicated time points. Representative images are shown.

degradable/destabilized BiFP or dBiFP, resulting in the pdBiFP-Linker vector (Supplemental Figure 1).

The highly degradable dBiFP can serve as a sensitive and dynamic transcript reporter of mouse lncRNA H19

As a proof-of-concept experiment, we generated a reporter construct containing mouse lncRNA H19 (or mH19) after the coding region of dBiFP, designated as dBiFP-H19 (Fig. 5A). It is expected that the dBiFP and mH19 should be transcribed as a chimeric transcript, in which dBiFP would be translated into the destabilized BiFP protein as a reporter. Potential siRNAs, microRNAs, other artificial modulatory RNAs, and/or RNA inhibitors that target mH19 would result in the decrease of the chimeric transcript and hence BiFP signal (Fig. 5A).

We stably introduced the dBiFP-H19 vector into HCT116 cells and found the expression level of mouse H19 was over 9-fold of the dBiFP control cells ($p < 0.01$) (Fig. 5B). Using our previously developed AdR-simH19 that specifically knocks down mouse H19 expressio,[46] we found that, when the dBiFP-H19 cells were infected with AdR-simH19, but not Ad-RFP control virus, the green fluorescence signal was significantly decreased at 36 h post infection, while no significant decrease in green fluorescence signal was observed in the control dBiFP cells (Fig. 5C—a). Quantitative analysis indicated that AdR-simH19-mediated H19 knockdown in the dBiFP-H19 cells effectively decreased the green fluorescence signal to 17.1% of the AdRFP infection group, or decreased by ~83%, compared with the AdRFP control ($p < 0.01$) (Fig. 5C—b). Accordingly, qPCR analysis revealed that AdR-simH19 infection knocked down the mouse H19 expression to 24.4% of the AdRFP infection control in the dBiFP-H19 cells ($p < 0.01$) (Fig. 5D), confirming that AdR-simH19 can effectively silence mouse H19 expression in the dBiFP-H19 cells. Thus, we designated the dBiFP vector as pdBIFP-Linker, which can be used as a generic vector for cloning any lncRNAs to generate dBiFP-lncRNA chimeric transcripts (Supplemental Figure 1). Taken together, our results strongly suggest that the dBiFP-H19 construct may serve as a sensitive yet dynamic transcript reporter to monitor the targeted inhibition of mouse H19 transcript.

Discussion

An ideal reporter for assessing dynamic real-time decrease of lncRNA transcript level should have a high signal level and yet a short half-life. In search for a sensitive high throughput system to identify potential negative regulators of lncRNAs, here we develop a dynamic and highly destabilized fluorescent protein-based reporter that can faithfully reflect the transcript levels of lncRNAs in human

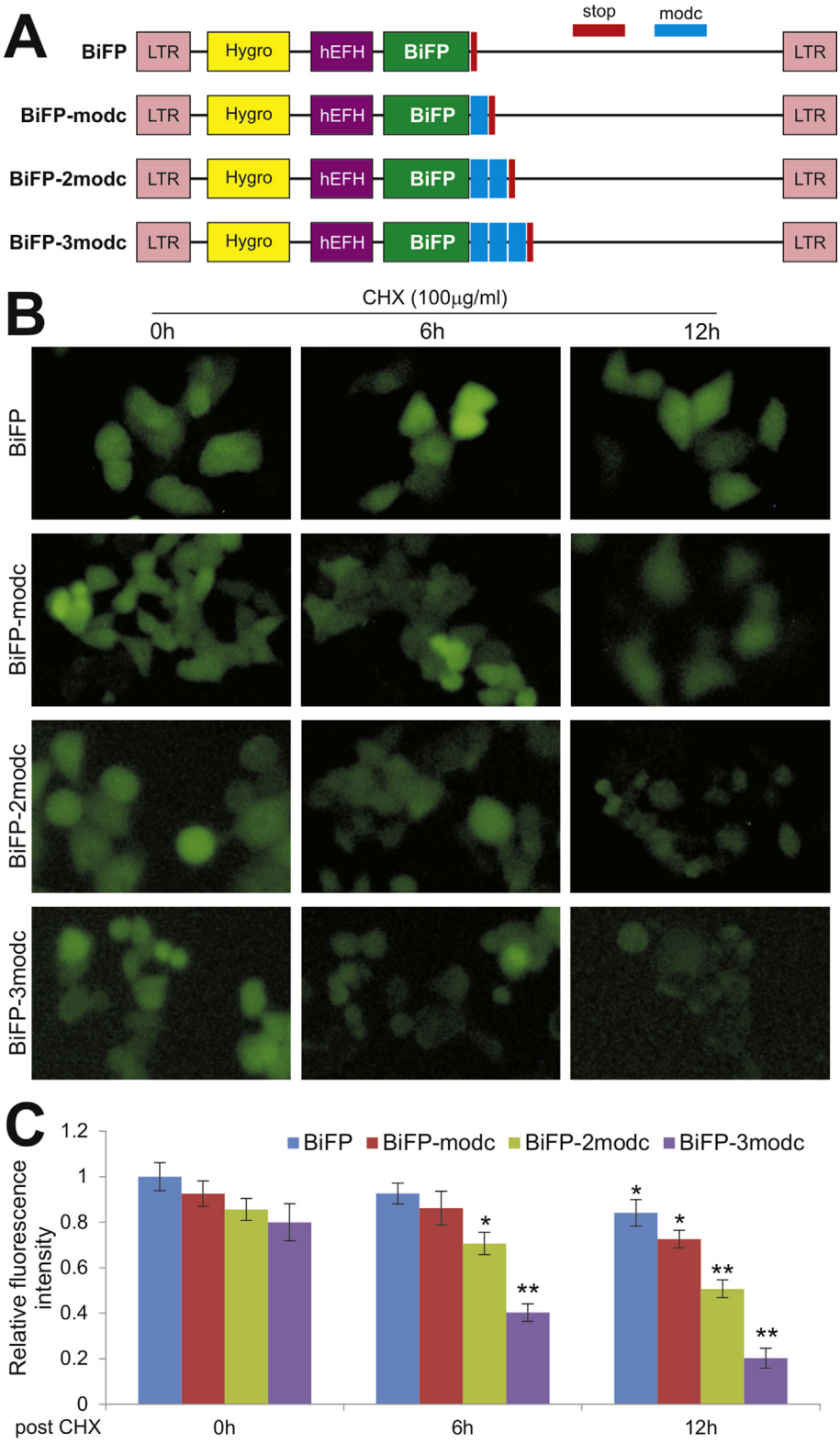

Figure 3 Characterization of the degradability of BiFP-modc C-terminal fusion proteins. (**A**) Schematic representation of destabilized BiFP constructs with zero to three copies of MODC PEST domain at the C-terminus of BiFP. The fusion constructs were generated and cloned in the pSEH retroviral vector, yielding pSEH-BiFP, pSEH-BiFP-modc, pSEH-BiFP-2modc, and pSEH-BiFP-3modc, respectively. (**B**) BiFP fusion constructs were used for retrovirus packaging and generating stable lines in HCT116 cells after hygromycin selection. Subconfluent stable lines were treated with CHX (100 μg/ml). Fluorescence signals were recorded at the indicated time points. Representative images are shown. (**C**) Quantitative analysis of the fluorescence signal for the CHX-treated stable lines shown in (**B**). "*" $p < 0.05$; "**" $p < 0.01$, compared with the BiFP signals at 0 h after CHX treatment of respective stable lines.

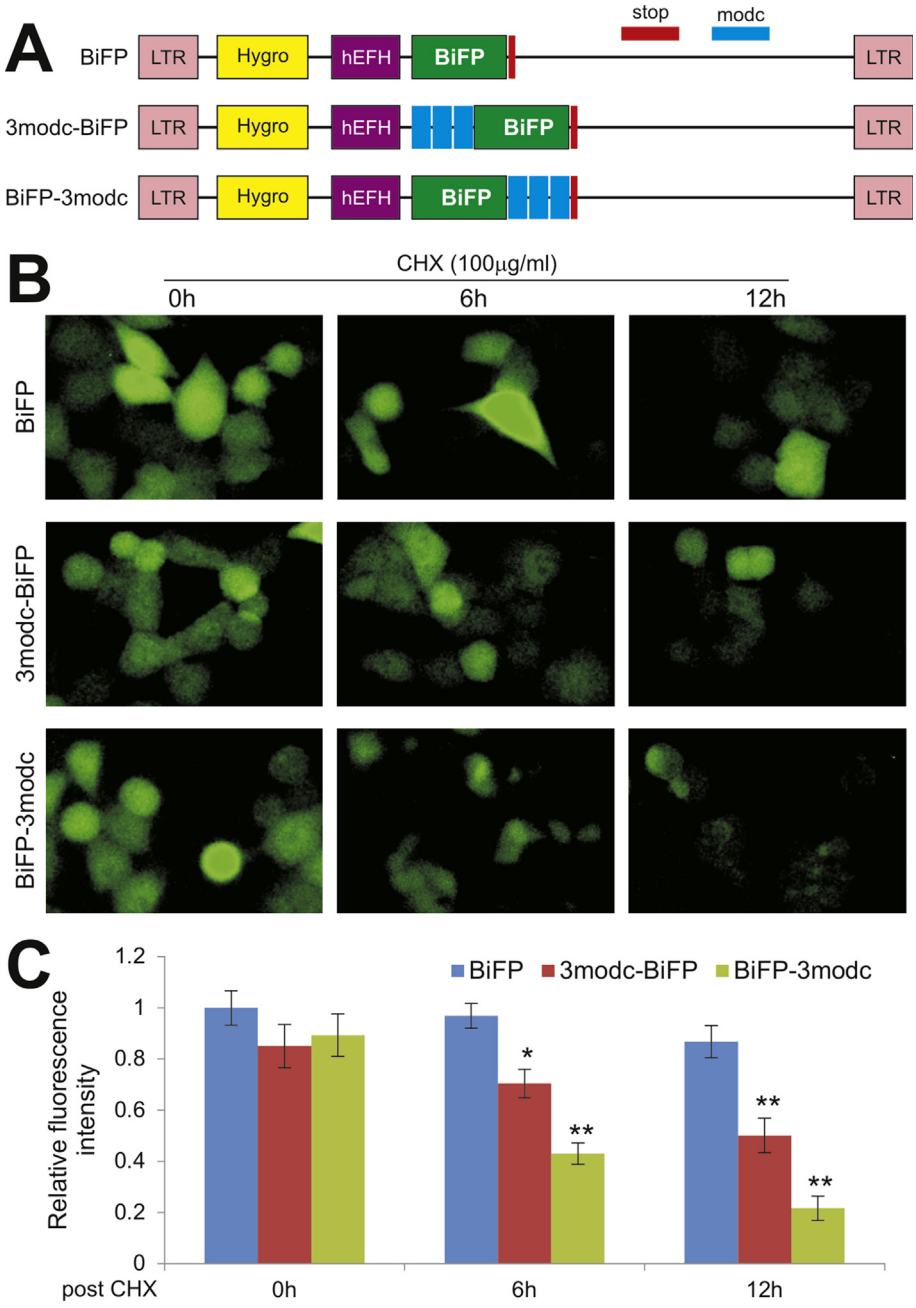

Figure 4 Degradability comparison of the BiFP fusion proteins containing the C-terminal or N-terminal MODC PEST domains. (**A**) Schematic representation of N-terminal and C-terminal fusion proteins of BiFP. The BiFP-3modc fusion construct is also designated as degradable BiFP or **dBiFP**. These constructs were generated in pSEH vector, resulting in pSEH-3modc-BiFP, pSEH-BiFP-3modc and pSEH-BiFP. (**B**) The retroviral vectors were used to generate stable HCT116 lines. Subconfluent stable lines were treated with CHX (100 μg/ml). Fluorescence signals were recorded at the indicated time points. Representative images are shown. (**C**) Quantitative analysis of the fluorescence signal for the CHX-treated stable lines shown in (**B**). "*" $p < 0.05$; "**" $p < 0.01$, compared with the BiFP signals at 0 h after CHX treatment of respective stable lines.

cancer cells. Specifically, we engineer the fluorescent fusion protein dBiFP by fusing three copies of the PEST destruction domain of mouse ornithine decarboxylase (MODC[39] to the C-terminal end of the codon-optimized bilirubin-inducible fluorescent protein. We show that dBiFP protein is highly destabilized and readily degradable, compared with the commonly-used eGFP. We further demonstrate that the dBiFP signal is effectively down-regulated when the dBiFP and mouse lncRNA H19 chimeric transcript is silenced by mouse H19-specific siRNAs. Thus, it is conceivable that the dBiFP fusion may serve as a sensitive and dynamic transcript reporter to monitor the targeted inhibitions of lncRNAs, which can be accomplished by microRNAs, synthetic RNA molecules and small molecule inhibitors in a high throughput fashion. It should be pointed out that the dBiFP reporter system can also be used to

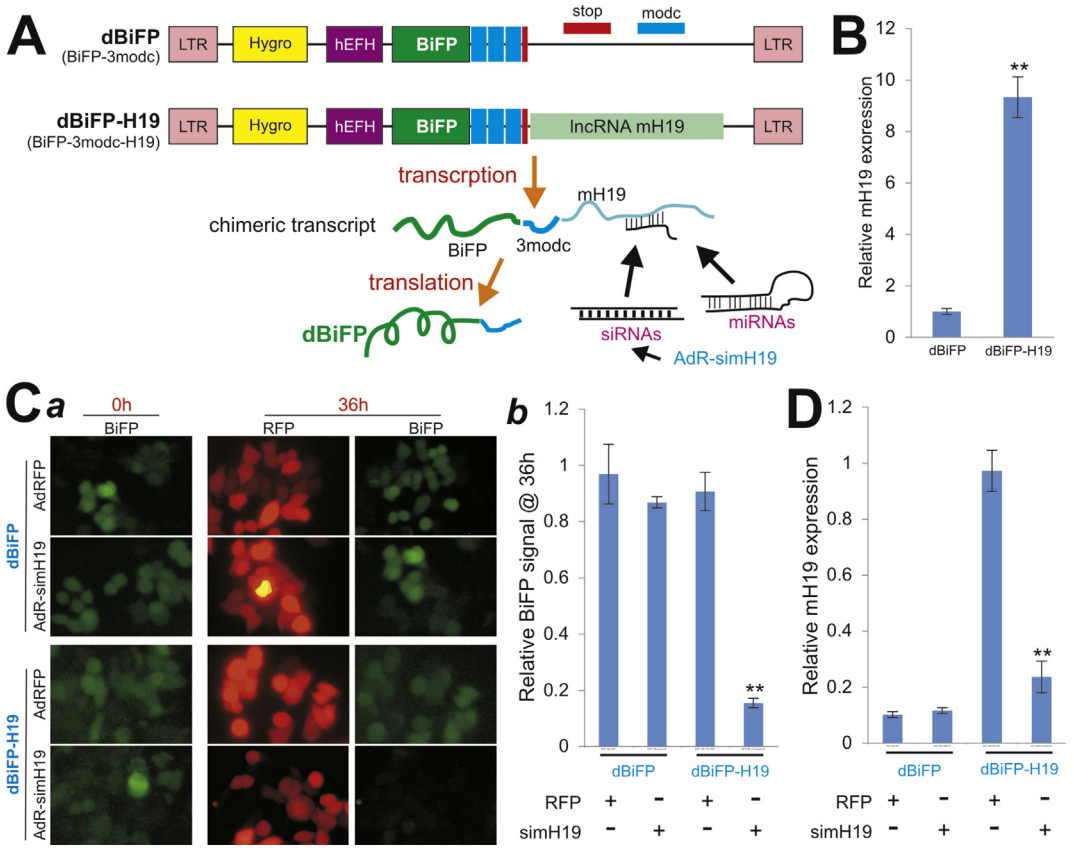

Figure 5 **The highly degradable dBiFP as a sensitive transcription reporter of lncRNA H19**. (**A**). Schematic representation of the construction of dBiFP-H19 transcriptional reporter. Mouse lncRNA H19 (mH19) was cloned into the downstream of the stop codon of the dBiFP coding region. It is expected a chimeric transcript of dBiFP-mH19 will be generated, which will be further translated into the highly degradable protein dBiFP. Targeting mH19 by siRNAs, miRNAs, naturally occurring or synthetic modulatory RNAs, or small molecule compounds may lead to a decrease in the chimeric transcript and thus the decrease in BiFP signal. As a proof-of-principle experiment, we use an adenoviral vector expressing mH19-specific siRNAs, AdR-simH19 to knockdown mH19 transcript. (**B**). Generation of a stable dBiFP-H19 reporter line from HCT116 cells. TqPCR analysis indicates the high expression of mouse H19 in the dBiFP-H19 HCT116 stable line ($p < 0.01$ compared with that of the control line dBiFP). (**C**). H19-specific siRNAs effectively down-regulate dBiFP expression in dBiFP-H19 cells. Subconfluent dBiFP and dBiFP-H19 cells were infected with AdR-simH19 or AdRFP. Fluorescence signals were recorded at 0 h and 36 h after infection (***a***). The BiFP fluorescence signal was quantitatively analyzed (***b***). "**", $p < 0.01$ compared the AdR-simH19 infection with that of AdRFP infection. (**D**). TqPCR analysis of mouse H19 in dBiFP-H19 cells upon AdR-simH19 silencing. Subconfluent dBiFP and dBiFP-H19 cells were infected with AdR-simH19 or AdRFP for 36 h. Total RNA was isolated and subjected to RT-PCR analysis. TqPCR assay was done in triplicate. "**" $p < 0.01$ when compared the expression level of AdR-simH19 infection with that of AdRFP infection.

assess changes in transcript levels of any protein-coding genes of interest.

Even though various reporter systems have been developed for various gene regulation or drug selection studies, sensitive reporters to assess the dynamic changes of lncRNA levels upon different inhibitor treatments are not readily available. We previously established an eGFP- target gene of interest reporter system to select for optimal siRNAs,[49,50] whereas the eGFP reporter is rather too stable and does not rapidly reflect the silencing efficiency of the target mRNAs. Nonetheless, most reporter systems are designed to assess promoter activity in regulating gene expression,[37,38] which is aimed at dissecting how cis-acting DNA sequences and trans-acting factors act in unison to control gene expression, not focusing on changes in the stability and/or level of the transcripts. Furthermore, it is important to recognize that traditional reporter assays measure protein levels or activities, but not RNA or transcript levels.

Numerous reporter genes have been use.[37,38,59,60] Nonetheless, there are several important criteria for selection of a promoter reporter gene. First, the reporter protein should be absent from the host, or easily distinguished from endogenous versions. Second, a simple, rapid, sensitive, and cost-effective assay should be available to detect the reporter protein. Third, the assay for the reporter protein should have a broad linear range to facilitate analysis of both large and small changes in promoter activity. Finally, expression of the gene must not alter the physiology of the recipient cells or organism. Commonly-used reporters include the isotopic assay-based reporters such as chloramphenicol acetyltransferase (CAT) and human growth hormone (hGH), the chemiluminescent

assay-based reporters such as firefly luciferase (FLuc) and β-galactosidase (or LacZ), and fluorescent protein-based assays such as GFP and mCherry fluorescent proteins.

Furthermore, significant progresses have been made for in vivo bioluminescence imaging of gene expression in order to understand the biological processes as they occur in living animals in real time.[61,62] One rapid and accessible technology for in vivo analysis employs internal biological sources of light emitted from luminescent enzymes, such as firefly luciferase, to label genes and cells detected by new generations of CCD cameras.[61,63,64] Such in vivo bioluminescence imaging and in vivo fluorescence imaging methods enable the real-time study of cell trafficking, various genetic regulatory elements in transgenic mice, and in vivo gene transfer, which greatly facilitate the functional analysis of a wide range of genes for their roles in health and disease.[62–64] Nonetheless, the choice of reporters is dictated, in most cases, by the assay requirements. For example, a reporter may be expressed in the cytoplasm or secreted to the culture medium. In general, fluorescent protein reporters are more suitable to locate in which cell or tissue the gene is activated or where in a cell the protein is expressed. Luciferases are more suitable to quantify how much and when the gene is expressed, but are usually not sensitive enough to pinpoint where the light is coming from. With the arrival of new cutting-edge molecular biology techniques, RNA transcripts in cells and/or tissues are routinely assessed by using qPCR and/or RNA-sequencing.

In this study, we demonstrate that the BiFP fluorescent protein exhibits many characteristics superior to that of the eGFP fusion protein in terms of fluorescent signal intensity, MODC-mediated degradability, and dynamic real-time responses to inhibitory modulators. Consistent with our findings was a recent report about the development of a novel protein domain that exhibits bilirubin-dependent stability and fluorescence based on the bilirubin-inducible fluorescent protein Una.[65] Furthermore, it has been recently reported that BiFP is associated with resistance to oxidative stress when coupled with bilirubin, suggesting that BiFP may provide the antioxidant activity to the cells as compared to eGFP.[66] This is an important feature as it is well established that when fluorophores (esp. GFP) are exposed to light, the process tends to generate reactive oxygen species (ROS) and can damage DNA, RNA, and proteins by oxidization.[67] Interestingly, consistent with that reported in the original publication,[45] we found that the fluorescence signal of BiFP-transduced cells is ligand-independent. This may be due to the wide presence of heme and/or bilirubin derivatives in cell culture medium. Nonetheless, it has been recently reported that the parental UnaG may adopt two distinct fluorescence states, UnaG in the apo-state (apoUnaG) and the holoUnaG, both of which are monomeric in aqueous solution.[68] Thus, it is conceivable that brighter BiFP/UnaG mutants may be genetically engineered as stronger fluorescent probes.

In summary, we engineer a highly destabilized fluorescent fusion protein dBiFP and show that dBiFP protein is highly degradable and dynamic, compared with the commonly-used eGFP. We further demonstrate that the dBiFP signal is effectively down-regulated when the dBiFP and mouse lncRNA H19 chimeric transcript is silenced by mouse H19-specific siRNAs. Thus, our results strongly suggest that the dBiFP fusion protein may serve as a sensitive and dynamic high-throughput transcript reporter to monitor the targeted inhibition of lncRNAs by microRNAs, synthetic RNA molecules and small molecule inhibitors.

Conflict of Interest

The authors declare no conflict of interest.

Acknowledgments

The reported work was supported in part by research grants from the National Institutes of Health (AT004418, DE020140 to TCH and RRR), the US Department of Defense (OR130096 to JMW), the Scoliosis Research Society (TCH and MJL), the National Key Research and Development Program of China (2016YFC1000803 and 2011CB707906 to TCH) and the National Natural Science Foundation of China (#81201916 to XW). ZZ was a recipient of protectorate fellowship from China Scholarship Council. This project was also supported in part by The University of Chicago Cancer Center Support Grant (P30CA014599) and the National Center for Advancing Translational Sciences of the National Institutes of Health through Grant Number UL1 TR000430. Funding sources were not involved in the study design; in the collection, analysis and interpretation of data; in the writing of the report; and in the decision to submit the paper for publication.

Appendix A. Supplementary data

Supplementary data related to this article can be found at https://doi.org/10.1016/j.gendis.2018.02.001.

References

1. Mattick JS, Makunin IV. Non-coding RNA. *Hum Mol Genet*. 2006; 15(Spec No 1):R17–R29.
2. Guttman M, Amit I, Garber M, et al. Chromatin signature reveals over a thousand highly conserved large non-coding RNAs in mammals. *Nature*. 2009;458(7235):223–227.
3. Carninci P, Kasukawa T, Katayama S, et al. The transcriptional landscape of the mammalian genome. *Science*. 2005; 309(5740):1559–1563.
4. Brosnan CA, Voinnet O. The long and the short of noncoding RNAs. *Curr Opin Cell Biol*. 2009;21(3):416–425.
5. Jacquier A. The complex eukaryotic transcriptome: unexpected pervasive transcription and novel small RNAs. *Nat Rev Genet*. 2009;10(12):833–844.
6. Kapranov P, Willingham AT, Gingeras TR. Genome-wide transcription and the implications for genomic organization. *Nat Rev Genet*. 2007;8(6):413–423.
7. Berretta J, Morillon A. Pervasive transcription constitutes a new level of eukaryotic genome regulation. *EMBO Rep*. 2009; 10(9):973–982.
8. Djebali S, Davis CA, Merkel A, et al. Landscape of transcription in human cells. *Nature*. 2012;489(7414):101–108.
9. Quinn JJ, Chang HY. Unique features of long non-coding RNA biogenesis and function. *Nat Rev Genet*. 2015;17(1):47–62.
10. Quinodoz S, Guttman M. Long noncoding RNAs: an emerging link between gene regulation and nuclear organization. *Trends Cell Biol*. 2014;24(11):651–663.

11. Johnsson P, Lipovich L, Grander D, Morris KV. Evolutionary conservation of long non-coding RNAs; sequence, structure, function. *Biochim Biophys Acta*. 2014;1840(3):1063—1071.
12. Hung T, Chang HY. Long noncoding RNA in genome regulation: prospects and mechanisms. *RNA Biol*. 2010;7(5):582—585.
13. St Laurent G, Wahlestedt C, Kapranov P. The Landscape of long noncoding RNA classification. *Trends Genet*. 2015;31(5):239—251.
14. Iyer MK, Niknafs YS, Malik R, et al. The landscape of long noncoding RNAs in the human transcriptome. *Nat Genet*. 2015;47(3):199—208.
15. Mellor J, Woloszczuk R, Howe FS. The interleaved genome. *Trends Genet*. 2016;32(1):57—71.
16. Geisler S, Coller J. RNA in unexpected places: long non-coding RNA functions in diverse cellular contexts. *Nat Rev Mol Cell Biol*. 2013;14(11):699—712.
17. Cech TR, Steitz JA. The noncoding RNA revolution-trashing old rules to forge new ones. *Cell*. 2014;157(1):77—94.
18. Grote P, Herrmann BG. Long noncoding RNAs in organogenesis: making the difference. *Trends Genet*. 2015;31(6):329—335.
19. Bohmdorfer G, Wierzbicki AT. Control of chromatin structure by long noncoding RNA. *Trends Cell Biol*. 2015;25(10):623—632.
20. Han P, Chang CP. Long non-coding RNA and chromatin remodeling. *RNA Biol*. 2015;12(10):1094—1098.
21. Sabin LR, Delas MJ, Hannon GJ. Dogma derailed: the many influences of RNA on the genome. *Mol Cell*. 2013;49(5):783—794.
22. Vance KW, Ponting CP. Transcriptional regulatory functions of nuclear long noncoding RNAs. *Trends Genet*. 2014;30(8):348—355.
23. Roberts TC, Morris KV, Weinberg MS. Perspectives on the mechanism of transcriptional regulation by long non-coding RNAs. *Epigenetics*. 2014;9(1):13—20.
24. Ma L, Bajic VB, Zhang Z. On the classification of long non-coding RNAs. *RNA Biol*. 2013;10(6):925—933.
25. Ulitsky I, Bartel DP. lincRNAs: genomics, evolution, and mechanisms. *Cell*. 2013;154(1):26—46.
26. Kim YJ, Maizel A, Chen X. Traffic into silence: endomembranes and post-transcriptional RNA silencing. *Embo J*. 2014;33(9):968—980.
27. Jonas S, Izaurralde E. Towards a molecular understanding of microRNA-mediated gene silencing. *Nat Rev Genet*. 2015;16(7):421—433.
28. Batista PJ, Chang HY. Long noncoding RNAs: cellular address codes in development and disease. *Cell*. 2013;152(6):1298—1307.
29. Migliore C, Giordano S. Resistance to targeted therapies: a role for microRNAs? *Trends Mol Med*. 2013;19(10):633—642.
30. Xia H, Hui KM. Mechanism of cancer drug resistance and the involvement of noncoding RNAs. *Curr Med Chem*. 2014;21(26):3029—3041.
31. Malek E, Jagannathan S, Driscoll JJ. Correlation of long non-coding RNA expression with metastasis, drug resistance and clinical outcome in cancer. *Oncotarget*. 2014;5(18):8027—8038.
32. Turner NC, Reis-Filho JS. Genetic heterogeneity and cancer drug resistance. *Lancet Oncol*. 2012;13(4):e178—e185.
33. Esteller M. Non-coding RNAs in human disease. *Nat Rev Genet*. 2011;12(12):861—874.
34. Taft RJ, Pang KC, Mercer TR, Dinger M, Mattick JS. Non-coding RNAs: Regulators of disease. *J Pathol*. 2010;220(2):126—139.
35. Wahlestedt C. Targeting long non-coding RNA to therapeutically upregulate gene expression. *Nat Rev Drug Discov*. 2013;12(6):433—446.
36. Kapusta A, Feschotte C. Volatile evolution of long noncoding RNA repertoires: mechanisms and biological implications. *Trends Genet*. 2014;30(10):439—452.
37. Alam J, Cook JL. Reporter genes: application to the study of mammalian gene transcription. *Anal Biochem*. 1990;188(2):245—254.
38. Kain SR, Ganguly S. Overview of genetic reporter systems. *Curr Protoc Mol Biol*. 2001 [Chapter 9]:Unit9 6:9.6.1—9.6.12.
39. Li X, Zhao X, Fang Y, et al. Generation of destabilized green fluorescent protein as a transcription reporter. *J Biol Chem*. 1998;273(52):34970—34975.
40. Wu N, Zhang H, Deng F, et al. Overexpression of Ad5 precursor terminal protein accelerates recombinant adenovirus packaging and amplification in HEK-293 packaging cells. *Gene Ther*. 2014;21(7):629—637.
41. Wei Q, Fan J, Liao J, et al. Engineering the rapid adenovirus production and amplification (RAPA) cell line to expedite the generation of recombinant adenoviruses. *Cell Physiol Biochem*. 2017;41(6):2383—2398.
42. He BC, Gao JL, Zhang BQ, et al. Tetrandrine inhibits Wnt/beta-catenin signaling and suppresses tumor growth of human colorectal cancer. *Mol Pharmacol*. 2011;79(2):211—219.
43. Huang E, Bi Y, Jiang W, et al. Conditionally immortalized mouse embryonic fibroblasts retain proliferative activity without compromising multipotent differentiation potential. *PLoS One*. 2012;7(2). e32428.
44. Huang E, Zhu G, Jiang W, et al. Growth hormone synergizes with BMP9 in osteogenic differentiation by activating the JAK/STAT/IGF1 pathway in murine multilineage cells. *J Bone Miner Res*. 2012;27(7):1566—1575.
45. Kumagai A, Ando R, Miyatake H, et al. A bilirubin-inducible fluorescent protein from eel muscle. *Cell*. 2013;153(7):1602—1611.
46. Liao J, Yu X, Hu X, et al. lncRNA H19 mediates BMP9-induced osteogenic differentiation of mesenchymal stem cells (MSCs) through Notch signaling. *Oncotarget*. 2017;8(32):53581—53601.
47. He TC, Zhou S, da Costa LT, Yu J, Kinzler KW, Vogelstein B. A simplified system for generating recombinant adenoviruses. *Proc Natl Acad Sci U S A*. 1998;95(5):2509—2514.
48. Luo J, Deng ZL, Luo X, et al. A protocol for rapid generation of recombinant adenoviruses using the AdEasy system. *Nat Protoc*. 2007;2(5):1236—1247.
49. Deng F, Chen X, Liao Z, et al. A simplified and versatile system for the simultaneous expression of multiple siRNAs in mammalian cells using Gibson DNA Assembly. *PLoS One*. 2014;9(11). e113064.
50. Luo Q, Kang Q, Song WX, et al. Selection and validation of optimal siRNA target sites for RNAi-mediated gene silencing. *Gene*. 2007;395(1-2):160—169.
51. Zhao C, Wu N, Deng F, et al. Adenovirus-mediated gene transfer in mesenchymal stem cells can be significantly enhanced by the cationic polymer polybrene. *PLoS One*. 2014;9(3). e92908.
52. Liao J, Wei Q, Fan J, et al. Characterization of retroviral infectivity and superinfection resistance during retrovirus-mediated transduction of mammalian cells. *Gene Ther*. 2017;24(6):333—341.
53. Kong Y, Zhang H, Chen X, et al. Destabilization of heterologous proteins mediated by the GSK3beta phosphorylation domain of the beta-catenin protein. *Cell Physiol Biochem*. 2013;32(5):1187—1199.
54. Huang J, Bi Y, Zhu GH, et al. Retinoic acid signalling induces the differentiation of mouse fetal liver-derived hepatic progenitor cells. *Liver Int*. 2009;29(10):1569—1581.
55. Zhu GH, Huang J, Bi Y, et al. Activation of RXR and RAR signaling promotes myogenic differentiation of myoblastic C2C12 cells. *Differentiation*. 2009;78(4):195—204.
56. Bi Y, Huang J, He Y, et al. Wnt antagonist SFRP3 inhibits the differentiation of mouse hepatic progenitor cells. *J Cell Biochem*. 2009;108(1):295—303.
57. Untergasser A, Cutcutache I, Koressaar T, et al. Primer3—new capabilities and interfaces. *Nucleic Acids Res*. 2012;40(15):e115.

58. Zhang Q, Wang J, Deng F, et al. TqPCR: a touchdown qPCR assay with significantly improved detection sensitivity and amplification efficiency of SYBR Green qPCR. *PLoS One*. 2015; 10(7). e0132666.
59. Schenborn E, Groskreutz D. Reporter gene vectors and assays. *Mol Biotechnol*. 1999;13(1):29—44.
60. Jiang T, Xing B, Rao J. Recent developments of biological reporter technology for detecting gene expression. *Biotechnol Genet Eng Rev*. 2008;25:41—75.
61. Contag CH, Bachmann MH. Advances in in vivo bioluminescence imaging of gene expression. *Annu Rev Biomed Eng*. 2002;4: 235—260.
62. Ray P, Gambhir SS. Noninvasive imaging of molecular events with bioluminescent reporter genes in living subjects. *Methods Mol Biol*. 2007;411:131—144.
63. Welsh DK, Noguchi T. Cellular bioluminescence imaging. *Cold Spring Harb Protoc*. 2012;2012(8).
64. Prescher JA, Contag CH. Guided by the light: visualizing biomolecular processes in living animals with bioluminescence. *Curr Opin Chem Biol*. 2010;14(1):80—89.
65. Navarro R, Chen LC, Rakhit R, Wandless TJ. A novel destabilizing domain based on a small-molecule dependent fluorophore. *ACS Chem Biol*. 2016;11(8):2101—2104.
66. Funahashi A, Komatsu M, Furukawa T, et al. Eel green fluorescent protein is associated with resistance to oxidative stress. *Comp Biochem Physiol C Toxicol Pharmacol*. 2016;181—182:35—39.
67. Dixit R, Cyr R. Cell damage and reactive oxygen species production induced by fluorescence microscopy: effect on mitosis and guidelines for non-invasive fluorescence microscopy. *Plant J*. 2003;36(2):280—290.
68. Shitashima Y, Shimozawa T, Kumagai A, Miyawaki A, Asahi T. Two distinct fluorescence states of the ligand-induced Green fluorescent protein UnaG. *Biophys J*. 2017;113(12): 2805—2814.